De La Cruz, R., Kanyinda-Malu, C., & Rodríguez, P. (2012). Phonons contribution to the infrared and visible spectra of II–VI semiconductor core-shell nanocrystals. *Physica E: Low-dimensional Systems and Nanostructures*, 44(9), 1868-1873.

DOI: 10.1016/j.physe.2012.05.018

Phonons contribution to the infrared and visible spectra of II–VI semiconductor core-shell nanocrystals

R.M. de la Cruz [a,*], C. Kanyinda-Malu [b], P. Rodríguez [a]

[a] Departamento de Física, Universidad Carlos III de Madrid, EPS. Avda. de la Universidad 30, 28911 Leganés (Madrid), Spain
[b] Departamento de Economía Financiera y Contabilidad II, Area de Matemáticas y Estadística, Universidad Rey Juan Carlos, FCJS, Paseo de los Artilleros s/n, 28032 Madrid, Spain

HIGHLIGHTS

- We investigate the bulk phonons contribution to the IR as well as the VIS spectra of II–VI nanoshells.
- We use Mie scattering theory by defining appropriate dielectric functions for the constitutive materials of the nanoshells.
- The effects of: (i) phonons, (ii) size of NCs and (iii) islanding medium are investigated in the IR and VIS range.
- Finite potential confinement is used to evaluate the exciton energy in effective mass approximation.

ARTICLE INFO

Article history:
Received 12 March 2012
Received in revised form
4 May 2012
Accepted 15 May 2012

ABSTRACT

We have investigated the phonons contribution in the infrared and visible optical properties in II–VI semiconductor nanoshells of type I. For this, we use Mie scattering theory by defining appropriate dielectric functions for the constitutive materials of the nanoshells. Indeed, for the core we have considered dielectric function taking into account the spatial confinement of the charge carriers along with the phonons contribution. For the shell, we have considered dielectric function similar to that used in bulk semiconductor. Independently of the core and shell sizes and the embedding medium, we obtain in the infrared (IR) spectra, three resonant peaks ascribed to the CdS stretching vibration, the longitudinal optical (LO)-CdS and surface optical (SO)-ZnS phonon modes, respectively. The increase of core and shell sizes induces a red shift of the Cd-S stretching vibration and the SO ZnS branches, while a blue-shift is obtained for the LO CdS branch. If the phonons contribution is not considered in the IR spectrum, the CdS stretching vibration is disappeared. On the other hand, in the visible (VIS) spectra, we obtain one sharp resonant peak related to the $1s_e$–$1s_h$ optical transition, whose localization is characterized by the core size, essential parameter to evaluate the exciton energy. Phonons contribution in the VIS range yields information about the exciton–phonon coupling in II–VI semiconductor nanoshells. When the embedding medium is glass, where the dielectric constants at high frequency of core, shell and islanding materials are similar, we obtain two effects on the IR as well as the VIS optical properties: (i) the phonon peaks (IR range) or the exciton peak (VIS range) are red-shifted, and (ii) the peaks intensities are greater. Therefore, in the light of these results, it can be concluded that the phonons contribution is primordial if the optical properties are investigated in the low-dimensional systems.

1. Introduction

In recent years, II–VI semiconductor core-shell type composite quantum dots (QDs) exhibit novel properties making them very attractive from both experimental and practical point of view. It was been shown that overcoating nanocrystallites improve the photoluminescence quantum yields by passivation of surface nonabsorbing recombination sites. Among examples of core-shell QDs reported in the literature, we can find CdS on CdSe and CdSe on CdS [1], ZnS grown on CdS [2,3], ZnS on the CdSe and CdSe on ZnS [4,5], ZnSe overcoated CdSe [6], CdSe coated ZnSe [7], ZnO on ZnS [8], etc.

Available theoretical models for QDs optical properties range from the formalism of light scattering of small particles based on polarizability of dielectric spheres to more sophisticated calculations [9–11]. The effects of charge carriers confinement on the self-polarization of the electron–hole pairs (excitons) in quantum

* Corresponding author. Tel.: +34 91 624 8733; fax: +34 91 624 8749.
E-mail addresses: rmc@fis.uc3m.es (R.M. de la Cruz), clement.kanyindamalu@urjc.es (C. Kanyinda-Malu).

dots were reported in spherical and non-spherical quantum dots. In many of these studies, the incorporation of the size-dependent functions is made following generalized Penn's model [12], or by including spatially smooth dielectric functions at the QD-surrounding material's interface [10]. In metallic nanoparticles for example, the effect of size on the dielectric function is often introduced through the size-dependent damping coefficient that accounts on different scattering mechanisms such as electron–electron, electron–phonon, surface and defect interactions [13].

In a previous work, we have investigated the optical properties of II–VI semiconductor nanoshells in a wide range of visible spectrum of light [14]. For that purpose, we applied Mie scattering theory by considering for core and shell, dielectric functions similar to that used in bulk semiconductors. As the investigated nanometric system is of type I, where the shell bandgap is larger than that of the core and both electrons and holes are confined in the core, it seems reasonable to consider as a dielectric function for the core which takes into account the confinement of charge carriers in order to correlate optical properties to nanoparticle sizes under appropriate boundary conditions. Webb et al. [15] and Fu et al. [16] have calculated the effective permittivity of the QD due to the ground-state exciton excited by an electromagnetic field. However, in those works, the authors have not investigated the optical properties in the infrared range, which is very interesting to elucidate the Raman spectra, neither the influence of phonons contribution in the dielectric response. Therefore, the aim of this work is to investigate the visible (VIS) and infrared (IR) spectra of II–VI semiconductor nanoshells taking into account the spatial confinement of charge carriers and the contribution of bulk optical phonon modes. Confinement of polar lattice vibrations is not considered herein since its effect is rather small compared with the confinement of charge carriers.

The paper is organized as follows. In Section 2, an outline of Mie scattering theory with the definition of the two contributions in core and shell dielectric functions is applied in spherical nanoshells. The implementation of the model in typical II–VI semiconductor nanoshells of type I along with a discussion of the results is given in Section 3. The main remarks and conclusion of this work will be given in Section 4.

2. Phonons contribution to the dielectric function and Mie scattering theory applied in core-shell nanocrystals

The system under investigation is a II–VI semiconductor spherical core-shell nanocrystal (NC) of type I. The NCs are characterized by a total radius R_s and a core of radius R_c surrounded by a shell layer (R_s-R_c), with their respective core and shell frequency-dependent dielectric functions ϵ_s and ϵ_c. As in nanoshells of type I, electrons and holes are confined in the core [17], the exciton is found to be localized in that region. To compute the phonons contribution to optical properties, we assume that the dielectric function for the core, ϵ_c, has two terms: the first one, obtained from the electric-dipole approximation, describes the quantum dot (QD) polarization due to the ground-state exciton as described in Refs. [15,16] and the second one, due to the bulk phonons contribution [18]. Calculations of electrons rate scattering values by confined longitudinal optical (LO) phonons in GaAs QDs yield phonon damping constants higher than the value considered in this work [19,20]. Therefore, in first approximation, the dielectric function of the core material should be restricted to

$$\epsilon_c(\omega)=\frac{8e^2}{V_c\epsilon_0 m_{ex,c}}\left[\frac{2\rho-1}{\omega_{ex,c}^2-\omega^2-i2\omega\gamma}\right]+\epsilon_{\infty,c}\left[1+\frac{\omega_{LO,c}^2-\omega^2}{\omega_{TO,c}^2-\omega^2-i\gamma_{ph}\omega}\right]. \tag{1}$$

In the above equation, $\omega_{TO,c}$ and $\omega_{LO,c}$ are the core transverse and longitudinal optical frequencies of the polar modes and γ_{ph} its damping constant. The remaining input parameters are defined as follows: $\epsilon_{\infty,c}$ is the core dielectric constant at high frequency, e the electron charge, V_c the core volume ($V_c=4\pi R_c^3/3$), ϵ_0 the free space permittivity. The core exciton reduced mass ($m_{ex,c}$), the linewidth (γ), which is considered in this work to be 3 meV and the parameter ρ (taken to be equal to 1 in the lossy resonance (absorption) approximation [15]) are other parameters that define the quantum dot dielectric function. Even if the introduction of phonons in our model can affect the linewidth dependence with the temperature (see [21]); however, this effect is not included hereafter. So we consider a small value of γ related to low temperatures, which is the experimental condition more usually investigated in the literature. In fact, $\omega_{ex,c}$ can be obtained from the approximate core exciton energy ($E_c=\hbar\omega_{ex,c}$), where we assume effective mass approximation by considering that carrier confinement energies are much greater than Coulomb interaction energy, which hence can be treated using perturbation approaches. Then, the exciton energy is written as

$$E_c=E_{g,c}+E(e)+E(h)+E(Coulomb). \tag{2}$$

$E_{g,c}$ is the intrinsic core band gap energy, while $E(e)$ and $E(h)$ are the electron and hole eigenenergies, respectively and $E(Coulomb)$ is the Coulomb interaction energy expressed as in Refs. [21,22]. In contrast to the Webb et al. model, where the exciton was calculated in the strong coupling regime (infinite barriers), we solve the envelope-function Schrödinger equation using a spherically symmetric confinement potential with finite barriers to find electron and hole eigenstates and their respective eigenvalues. Due to this symmetry, the electron and hole wave functions only depend on the radial coordinate r. For more details, see for example Refs. [21,23].

For the shell material, we use the bulk-like semiconductor dielectric function, ϵ_s, with its plasmons and phonons contributions as described in Ref. [18]; i.e.,

$$\epsilon_s(\omega)=\epsilon_{\infty,s}\left[1+\frac{\omega_{LO,s}^2-\omega^2}{\omega_{TO,s}^2-\omega^2-i\gamma_{ph}\omega}-\frac{\omega_p^2}{\omega^2+i\gamma_p\omega}\right]. \tag{3}$$

Once again, $\omega_{TO,s}$ and $\omega_{LO,s}$ are the shell transverse and longitudinal optical frequencies of the polar modes and γ_{ph} its damping constant, while $\epsilon_{\infty,s}$ is the high-frequency dielectric constant of shell. On the other hand, ω_p and γ_p are, respectively, the frequency and damping constant of plasmons for shell material. To complete the description of our nanostructure, both the core and shell materials are embedded in an insulating medium, whose non-frequency dependent dielectric function is denoted by ϵ_e.

Once the dielectric functions are well established, we apply the Mie scattering theory to the above defined core-shell nanocrystals as extensively reported in the literature [13,14]. To summarize our calculations, we will only remind hereafter the expressions of absorption and scattering cross-sections. Indeed, the absorption cross-section is given as follows [13]:

$$\sigma_{abs}=\frac{8\pi^2\sqrt{\epsilon_e}}{\lambda}R_s^3\mathrm{Im}\left(\frac{\epsilon_s\epsilon_a-\epsilon_e\epsilon_b}{\epsilon_s\epsilon_a+2\epsilon_e\epsilon_b}\right) \tag{4}$$

and for the scattering cross-section we have [13]

$$\sigma_{sca}=\frac{128\pi^5}{3\lambda^4}\epsilon_e^2R_s^6\left|\frac{\epsilon_s\epsilon_a-\epsilon_e\epsilon_b}{\epsilon_s\epsilon_a+2\epsilon_e\epsilon_b}\right|^2. \tag{5}$$

In the above equations ϵ_a and ϵ_b are defined as

$$\epsilon_a=\epsilon_c(3-2P)+2\epsilon_sP, \tag{6}$$

$$\epsilon_b=\epsilon_cP+\epsilon_s(3-P), \tag{7}$$

being

$$P = 1-(R_c/R_s)^3. \quad (8)$$

On the other hand, the extinction cross-section (σ_{ext}) is defined as $\sigma_{ext} = \sigma_{abs} + \sigma_{sca}$ [24]. Finally, the absorption, scattering and extinction coefficients are obtained by dividing their respective cross-sections by the total core-shell nanostructure volume.

3. Results and discussion

To illustrate our results, we apply the Mie scattering theory in typical II–VI semicondcutor core-shell nanocrystals such as CdS/ZnS, where the effects of (i) phonons contribution, (ii) size of core-shell nanocrystals and (iii) islanding medium will be investigated on the IR and VIS optical spectra. As the nanocrystals have nanometric sizes, the extinction is mainly due to absorption processes, accordingly to the optical properties in typical low-dimensional systems [25]. Indeed, the extinction (extinction coefficient multiplied by the nanocrystal thickness) will be shown as a function of the wavenumber (IR range) or the wavelength (VIS range). In order to emphasize the phonons contribution in the optical response, we will show in a same figure the extinction evaluated with and without phonons contribution to the core dielectric function. Values of the different constants for CdS, ZnS and insulating media are given in Table 1 [26–29].

As our aim is to clarify the discussion of the different effects, we present in separate subsections the optical properties of CdS/ZnS nanoshells in the IR and VIS ranges, respectively.

3.1. Extinction of CdS/ZnS nanoshells in the IR range

Within this range, we will mainly investigate the different lattice vibrations of the core and shell materials. Fig. 1 shows the extinction for CdS/ZnS/polyethylene nanoshells as a function of the wavenumber with radii $R_c=3$ nm and $R_s=5$ nm. When we consider the phonons contribution to the core dielectric function, we obtain three resonant peaks located around 241 cm^{-1}, 286 cm^{-1} and 306 cm^{-1}, respectively.

The peak around 241 cm^{-1} is usually ascribed to the stretching of CdS vibration [30]. Milekhin et al. [31] have demonstrated that the stretching of CdS vibration confirms the CdS quantum dots (QDs) formation in the Landmuir–Blodgett matrix. The second peak of 286 cm^{-1} is nearly close to the experimental value of 297 cm^{-1} obtained in CdS QDs with Raman spectroscopy [31]. Milekhin et al. [31] ascribed the value of 297 cm^{-1} to CdS LO phonons; however, this value is less than that of the LO phonon in bulk CdS (303 cm^{-1}) [32]. The difference between the phonon frequencies in the structures with QDs and the frequencies in the bulk materials can be explained by the effect of optical phonons localization in QDs, for a review of this phenomenon, see for example [33,19]. Notice that the difference between 286 cm^{-1} and 297 cm^{-1} could find explanation in a different way. The LO phonons are confined in CdS/ZnS/polyethylene NCs compared to that of CdS QDs in the Landmuir–Blodgett matrix. Han et al. [34] recently reported values around 280 cm^{-1} in CdS NCs with a radius of 2 nm. These values were obtained by DFT.

Table 1
Different parameters of the materials used in this work. In our approach, the exciton reduced mass for ZnS is not necessary to evaluate its dielectric function.

Parameters	CdS	ZnS	Polyethylene	Glass
ϵ_∞	5.5	5.2	2.3	4.64
ω_{LO} (cm^{-1})	300	349	–	–
ω_{TO} (cm^{-1})	233	269	–	–
m_e^*	0.19	–	–	–
m_h^*	0.8	–	–	–
ω_p (cm^{-1})	–	69.7	–	–
γ (cm^{-1})	–	27.1	–	–
γ_{ph} (cm^{-1})	8.5	8.5	–	–

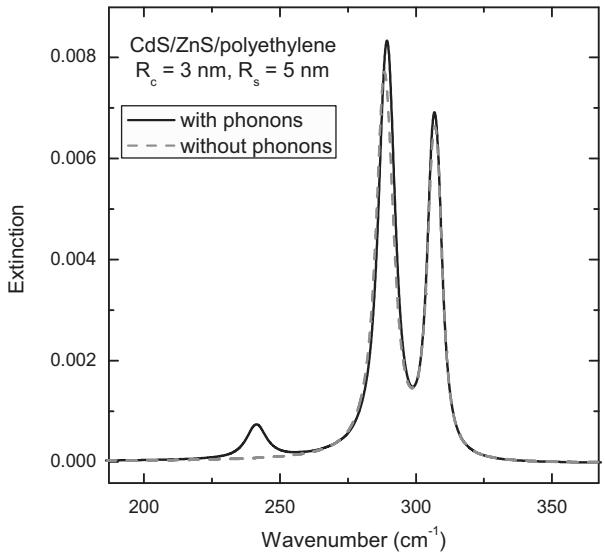

Fig. 1. Extinction for CdS/ZnS/polyethylene nanoshells as a function of the wavenumber, with (solid line) and without (dashed line) phonons contribution in the core dielectric function with radii $R_c=3$ nm and $R_s=5$ nm.

The peak at 306 cm^{-1} can be related to the SO ZnS phonon modes. The calculated frequency by means of dielectric continuum model in spherical ZnS QDs is 316 cm^{-1}, which agrees with the experimental value obtained in Raman spectra [31]. The plausible difference between our value of 306 cm^{-1} and 316 cm^{-1} could derive from the fact that we use a ZnS nanoshell instead of a ZnS QD in our calculations. In fact, in one of our previous work, we obtained by means of the dielectric continuum model values of the ZnS SO modes around 303 cm^{-1} in CdS/ZnS/polyethylene nanoshells when the ratio R_s/R_c is approximately 1.7 [35] (we are using similar sizes in the present work). In our IR spectra, the absence of the ZnS-related TO and LO phonons frequencies agrees quite well with the results of Raman spectra and IR reflection spectra for small ZnS QDs [31]. Milekhin et al. [31] argued that for small-sized QDs, the ratio of the surface atoms to the bulk atoms is relatively large; therefore, when the number of surface atoms becomes comparable or even larger than that in the bulk of the QDs, the contribution of the surface layers to the Raman scattering becomes significant. Conversely, when we do not take into account the phonons contribution to the core dielectric function, the peak at 241 cm^{-1} related to the stretching of CdS vibration disappeared. Then, we can postulate that the inclusion of phonons contribution in theoretical calculations is primordial in order to reproduce the experimental Raman spectra in CdS/ZnS nanoshells. If the embedding material of the NC is glass, we observe that the resonant peaks are red-shifted toward 240 cm^{-1}, 285 cm^{-1} and 304 cm^{-1}, respectively, along with an increase of their intensities, becoming somehow the double of that observed in polyethylene-embedded structures (see Fig. 2). These two effects were previously reported in the literature in II–VI semiconductor nanoshells when the core, shell and embedding materials have similar dielectric constants at a high frequency [14]. It seems that the proximity among the three dielectric constant values entail a plausible cooperative phenomenon in the average dielectric response versus the incident light, increasing consequently the extinction. Again, when we neglected

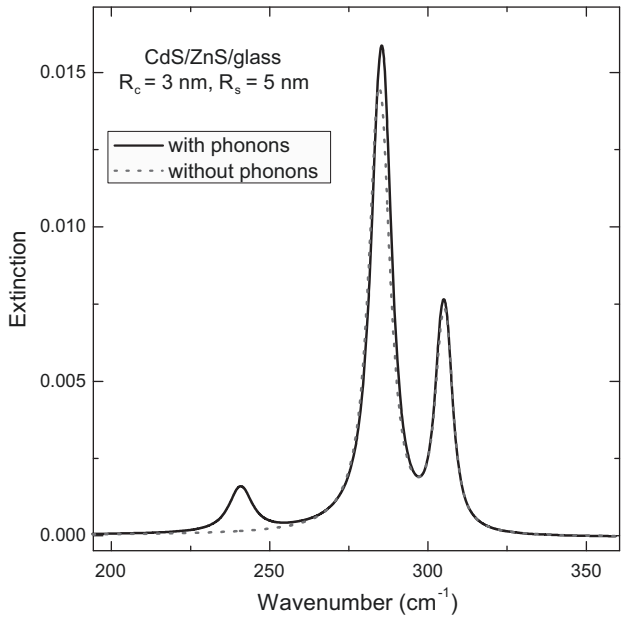

Fig. 2. Extinction for CdS/ZnS/glass nanoshells as a function of the wavenumber, with (solid line) and without (dashed line) phonons contribution in the core dielectric function with radii R_c=3 nm and R_s=5 nm.

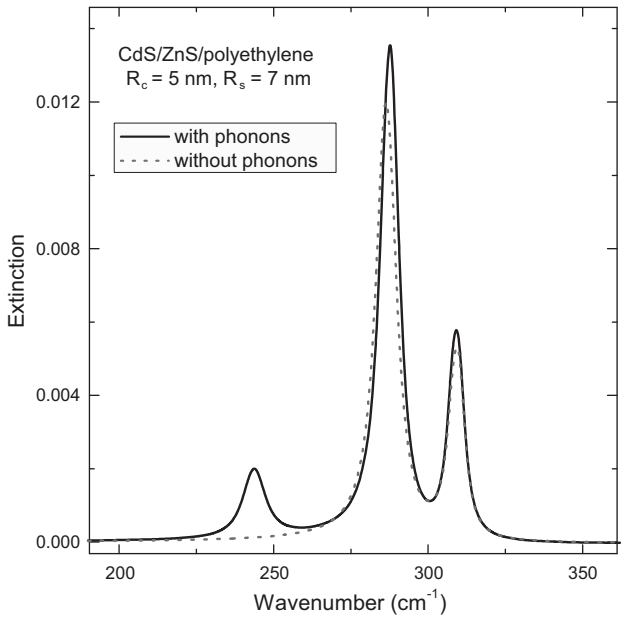

Fig. 3. Extinction for CdS/ZnS/polyethylene nanoshells as a function of the wavenumber, with (solid line) and without (dashed line) phonons contribution in the core dielectric functions with radii R_c=5 nm and R_s=7 nm.

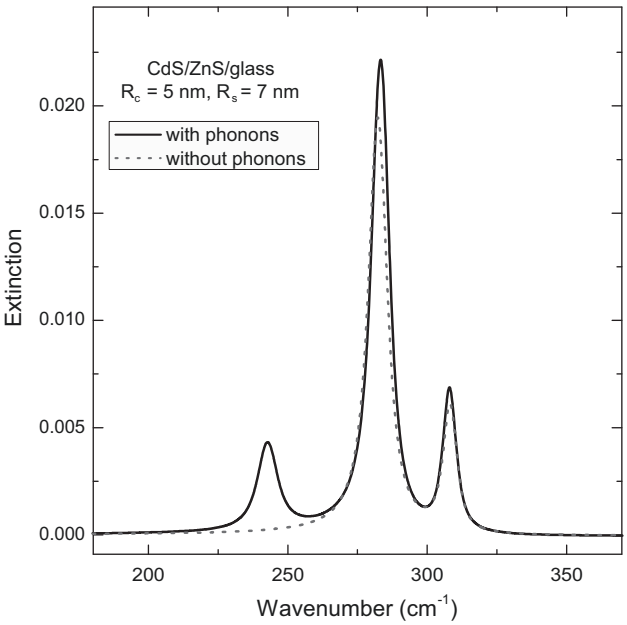

Fig. 4. Extinction for CdS/ZnS/glass nanoshells as a function of the wavenumber, with (solid line) and without (dashed line) phonons contribution in the core dielectric function with radii R_c=5 nm and R_s=7 nm.

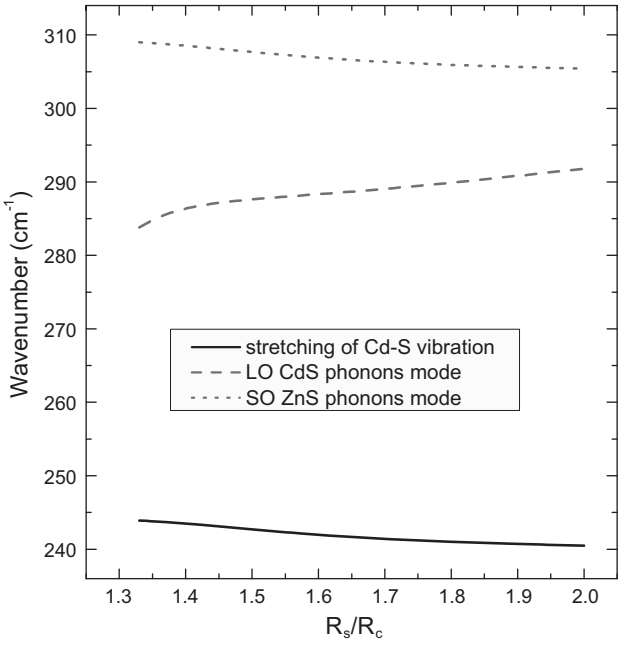

Fig. 5. Dependence of the phonons branches for CdS/ZnS/polyethylene nanoshells with the ratio R_s/R_c.

the phonons contribution to the core dielectric function, the resonant peak ascribed to the CdS stretching vibration disappeared.

To investigate the size effects on the IR spectra, we present in Figs. 3 and 4 the extinction of CdS/ZnS nanoshells as a function of the wavenumber with radii R_c=5 nm and R_s=7 nm embedded in polyethylene and glass, respectively. For both insulating media, we find that the three resonant peaks are slightly shifted towards 1 or 2 cm^{-1}, shift which can be explained in terms of the phonon localization in low-dimensional systems [33,19]. In order to clarify the size effects on the IR spectra, we show in Fig. 5 the behavior of three resonant phonon peaks as a function of the ratio R_s/R_c. We should quote that the most significative shift is that related to the LO CdS phonon modes branch, with a value around 2.8% over the investigated ratio R_s/R_c. Another effect to mention in the IR spectra is that the intensities of these resonant peaks are greater when the radii increase. This feature was previously reported in CdS/ZnS nanoshells [14]. Again, we obtain that the absence of the phonons contribution to the core dielectric function entails the suppression of the peak related to the stretching of CdS vibration. On the other hand, replacing the polyethylene by glass in embedding medium provides similar effects in the IR optical spectra than those obtained when the nanoshell radii were R_c=3 nm and R_s=5 nm.

In the light of the above results, we can conclude that: (i) the inclusion of phonons contribution to the core dielectric function

of II–VI semiconductor nanoshells is essential to evaluate the lattice vibrations effect on the IR spectra of the nanoshells; and (ii) the size effects are noticeable in the phonon localization in these systems giving rise to small modifications in the position of their resonant frequencies when the size changes.

3.2. Extinction in CdS/ZnS nanoshells in the VIS range

Within this range, we will mainly investigate the size effects on the $1s_e$–$1s_h$ optical transition. By considering the phonons contribution to the core dielectric function, we will investigate the plausible exciton–phonon coupling in these CdS/ZnS nanoshells. Fig. 6 shows the extinction for CdS/ZnS/polyethylene nanoshells as a function of the wavelength with radii $R_c=3$ nm and $R_s=5$ nm. Independently of the phonons contribution to the core dielectric function, we obtain a very sharp resonant peak located at 445 nm (without phonons) and at 452 nm (with phonons). From Eq. (2), which describes the core exciton energy, we can attribute these peaks to the $1s_e$–$1s_h$ optical transition in CdS cores of radius 3 nm. The shift between the two peaks around 7 nm corresponds to a difference of energy around 36 meV. This value could be attributed to the energy of the exciton–phonon coupling. The polaron self-energy in III–V semiconductor nanostructures is of the same order of magnitude, although it is slightly lesser [36]. Indeed, we can infer that the value of 36 meV is the coupling energy between exciton and LO- and SO-phonon modes in CdS/ZnS NCs. As the peak intensity is smaller when the phonons contribution is taken into account, we could deduce that the lattice vibrations would screen the charge carriers in the nanoshells, diminishing consequently the interaction strength between the incident light and the electric field due to the charge carriers.

In order to investigate the size effects, we show in Fig. 7 the extinction for CdS/ZnS/polyethylene nanoshells as a function of the wavelength with radii $R_c=5$ nm and $R_s=7$ nm. Similar to the above investigated size, we obtain a very sharp resonant peak located at 485 nm (without phonons) and at 489 nm (with phonons), which can be related to the $1s_e$–$1s_h$ optical transition

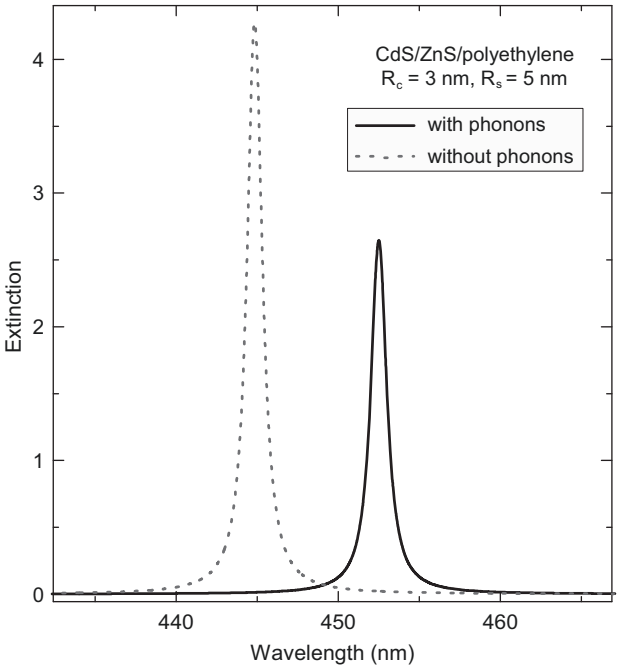

Fig. 6. Extinction for CdS/ZnS/polyethylene nanoshells as a function of the wavelength, with (solid line) and without (dashed line) phonons contribution in the core dielectric function with radii $R_c=3$ nm and $R_s=5$ nm.

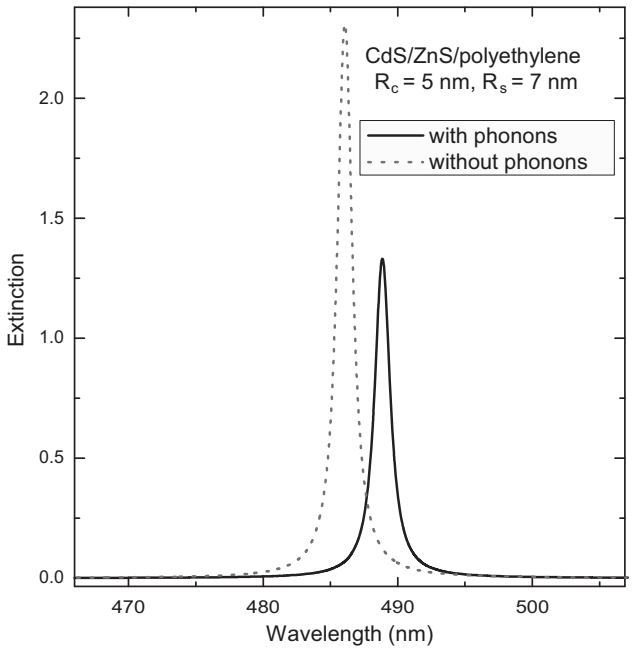

Fig. 7. Extinction for CdS/ZnS/polyethylene nanoshells as a function of the wavelength, with (solid line) and without (dashed line) phonons contribution in the core dielectric function with radii $R_c=5$ nm and $R_s=7$ nm.

in CdS cores of radius 5 nm. As the core radius is greater, the exciton energy is lesser, then a red-shift of the resonant peaks is obtained. Again, the shift of approximately 4 nm between the peaks obtained with and without phonons contribution corresponds to a difference of energy around 21 meV, which is associated to the energy of the exciton–phonon coupling. By comparing with the above value of 36 meV, we can deduce that the exciton–phonon coupling has a dependence on the nanoshell size feature which is previously reported in the literature [37]. In fact, Nomura et al. [37] attributed a decreasing Huang–Rhys parameter in II–VI semiconductor microcrystals, when the NC size increases, to a reduction of the exciton–phonon coupling, such as we have deduced from the decreasing exciton–phonon coupling energy when the core size increases. Also, although it is not shown herein, the embedding material effects on the VIS spectra are similar to that obtained in the IR spectra; i.e, when the islanding medium is glass, we obtain two effects: (i) a red-shift of the resonant peaks related to excitons and (ii) an increasing of the intensities peaks. Therefore, it seems that if an extinction decreasing in nanoshells is wanted for some technological applications, these systems should be fabricated with materials whose dielectric constants were rather different. Conversely, the exciton–phonon coupling is not affected by the islanding material change. Indeed, we obtain for CdS/ZnS/glass nanoshells with radii $R_c=3$ nm and $R_s=5$ nm, a value of 36 meV for the exciton–phonon coupling energy, equal value than for the previous investigated case when the embedding medium was polyethylene.

In the light of the above results, we can conclude for the VIS spectra of II–VI semiconductor nanoshells that the inclusion of phonons contribution to the core dielectric function is necessary to remark the experimental evidence of exciton–phonon coupling.

4. Conclusions

In summary, phonons contribution on the IR and VIS optical spectra of II–VI semiconductor nanoshells of type I has been investigated by means of the Mie scattering theory by defining appropriate dielectric functions for the constitutive materials of

the nanoshells. In fact, for the core we have considered dielectric function taking into account the spatial confinement of the charge carriers along with the phonons contribution. For the shell, we have considered dielectric function similar to that used in bulk semiconductor. Indeed, bulk phonons contribution provides features of interest for optical properties of II–VI semiconductor nanoshells:

1. Unlike the difference in the core and shell sizes and the embedding material, three resonant peaks are observed over the IR range when the phonons contribution is taken into account. Each peak corresponds to CdS stretching vibration, LO-CdS and SO-ZnS phonon modes, respectively.
2. In the IR range, the increase of the ratio R_s/R_c yields a red shift of CdS stretching vibration and SO-ZnS phonon modes, while for LO-CdS phonon modes a blue shift is observed.
3. In the VIS range, we obtain a very sharp peak related to the $1s_e$–$1s_h$ optical transition in CdS core. This peak is red-shifted when the core size increases, result which is consistent with the fact that the exciton energy decreases for increasing core sizes.
4. The bulk phonons contribution in VIS range is noticeable yielding an appropriate evaluation of the exciton–phonon self-energy in II–VI nanoshells.
5. When the islanding medium is glass, where the dielectric constants at high frequency of the core, shell and embedding materials are similar, we obtain two effects in the IR as well as the VIS optical spectra: (i) the phonons peaks (IR range) or the exciton peaks (VIS range) are red shifted, and (ii) the peaks intensities are greater.
6. Confinement effects of charge carriers are more significative than those of the lattice vibration modes when the nanoshell size is diminished.

Finally, our study can constitute an interesting information when the lattice vibrations and their coupling with excitons are investigated in II–VI semiconductor nanoshells.

References

[1] M.A. Malik, P. O'Brien, N. Revaprasadu, Chemical Material 14 (2002) 2004.
[2] J.S. Steckel, J.P. Zimmer, S. Coe-Sullivan, N.E. Stott, V. Bulovic, M.D. Bawendi, Angewandte Chemie International Edition 43 (2004) 2154.
[3] A. Datta, S.K. Panda, S. Chaudhuri, Journal of Physical Chemistry 111 (2007) 17260.
[4] J.-H. Song, T. Atay, S. Shi, H. Urabe, A.V. Nurmiko, Nano Letters 5 (2005) 1557.
[5] Y. Ma, H.X. Bai, C. Yang, X.R. Yang, Analyst 130 (2005) 1386.
[6] D.A. Bussian, S.A. Crooker, M. Yin, M. Brynda, AL. Efros, V.I. Kliomov, Nature Materials 8 (2009) 35.
[7] P. Reiss, J. Bleuse, A. Pron, Nano Letters 2 (2002) 781.
[8] J. Schrier, D.O. Demchenko, L.-W. Wang, A.P. Alivisatos, Nano Letters 7 (2007) 2377.
[9] A. Francheschetti, H. Hu, L.W. Wang, A. Zunger, Physical Review B 60 (1999) 1819.
[10] P.G. Bolcatto, C.R. Proetto, Physica Status Solidi (B) 220 (2000) 220.
[11] G. Bester, A. Zunger, Physical Review B 68 (2003) 73309.
[12] L.-W. Wang, A. Zunger, Physical Review Letters 73 (1994) 1039.
[13] R.D. Averitt, S.L. Westcott, N.J. Halas, Journal of the Optical Society of America B 16 (1999) 1824.
[14] R.M. de la Cruz, C. Kanyinda-Malu, J. Iñarrea, F.J. Clares, S.N. Santalla, Physica Status Solidi (C) 6 (2009) 2097.
[15] K.J. Webb, A. Ludwig, Physical Review B 78 (2008) 153303.
[16] Y. Fu, L. Thylén, H. Agren, Nano Letters 8 (2008) 1551.
[17] P. Reiss, M. Protière, L. Li, Small 5 (2009) 154.
[18] F. Demangeot, J. Frandon, M.A. Renucci, C. Meny, O. Briot, R.L. Aulombard, Journal of Applied Physics 82 (1997) 1305.
[19] R.M. de la Cruz, S.W. Teitsworth, M.A. Stroscio, Superlattices and Microstructures 13 (1993) 481.
[20] R.M. de la Cruz, Superlattices and Microstructures 16 (1994) 427.
[21] R.M. de la Cruz, C. Kanyinda-Malu, Physica E 44 (2012) 1250.
[22] G. Jia, Y. Wang, J. Yao, Optoelectronics and Advanced Materials: Rapid Communications 4 (2010) 2080.
[23] A. Piryatinski, S.A. Ivanov, S. Tretiak, V.I. Klimov, Nano Letters 7 (2007) 108.
[24] J.M. Oliva, S.K. Gray, Chemical Physics Letters 379 (2003) 325.
[25] H.C. Hulst, Scattering by Small Particles, Dover, New York, 1981.
[26] J. Brandrup, E.K. Immergut (Eds.), Polymer Handbook, Wiley, New York, 1989.
[27] Landolt-Börnstein, Numerical Data and Functional Relationships in Science and Technology, Springer, Berlin, 1982.
[28] P.M. Nikolic, Z. Dinovic, K. Radulovic, D. Vasijevic-Radovic, S. Duric, P. Mihajlovic, D.I. Siapkas, T.T. Zorba, in: Proceedings of the 22nd International Conference on Microelectronics, MIEL, Nis, Serbia, 2000, vol. 1.
[29] A.G. Rolo, L.G. Vieira, M.J.M. Gomes, J.L. Ribeiro, M.S. Belsley, M.P. dos Santos, Thin solid films 312 (1998) 348.
[30] R. Seoudi, M. Kamal, A.A. Shabaka, E.M. Abdelrazek, W. Eisa, Synthetic Metals 160 (2010) 479.
[31] A.G. Milekhin, R.K. Roy, A.K. Pal, Journal of Physics D: Applied Physics 35 (2002) 2198.
[32] L.E. Brus, Journal of Chemical Physics 80 (1984) 4403.
[33] C. Trallero-Giner, R. Pérez-Alvárez, F. García-Moliner, Long Wave Polar Modes in Semiconductor Heterostructures, Pergamon, Oxford, 1998.
[34] P. Han, G. Bester, Physical Review B 85 (2012) 041306-1.
[35] I. López, C. Kanyinda-Malu, R.M. de la Cruz, Physica Status Solidi (A) 203 (2006) 1370.
[36] C. Kanyinda-Malu, R.M. de la Cruz, in: Recent Research Developments in Crystal Growth, Part II, vol. 4, 2005, India, pp. 269-353. ISBN:81-7895-172-X.
[37] S. Nomura, T. Kobayashi, Physical Review B 45 (1992) 1305.